Haipeng et al., *Cogent Physics* (2016), 3: 1244244
http://dx.doi.org/10.1080/23311940.2016.1244244

cogent physics

MATERIALS SCIENCE | RESEARCH ARTICLE

Preparation and thermal properties of Sm_2AlTaO_7

Yu Haipeng[1], Chen Xiaoge[2], Zhang Hongsong[3,4]*, Zhang Haoming[4], Zhao Yongde[3], Liu Yanxu[4] and Tang An[4]

Received: 27 July 2016
Accepted: 23 September 2016
First Published: 05 October 2016

*Corresponding author: Zhang Hongsong, Institute of Chemistry, Henan Academy of Sciences, Zhengzhou 450007, China; School of Mechanical Engineering, Henan Institute of Engineering, Zhengzhou 450002, China
E-mails: zhsandchen@126.com, zhs761128@163.com

Reviewing editor:
Rajeev Ahuja, Uppsala University, Sweden

Additional information is available at the end of the article

Abstract: In this work, the Sm_2AlTaO_7 was synthesized by solid reaction method, and its phase composition, microstructure, and thermophysical properties were investigated. XRD results show that pure Sm_2AlTaO_7 with single pyrochlore-type structure is prepared successfully. The thermal conductivity of Sm_2AlTaO_7 at 1,273 K is about 1.13 W m^{-1} K^{-1}, which is much lower than that of YSZ. The low thermal conductivity can be attributed to the phonon scattering caused by substituting atoms. Its thermal expansion coefficient is lower than that of $Sm_2Ce_2O_7$, but close to that of YSZ. There is no phase transformation occurred between 293 and 1,673 K. The excellent thermophysical property means that the Sm_2AlTaO_7 has potential to be used as candidate ceramic material for thermal barrier coatings.

Subjects: Coatings & Thin Films-Materials Science; Materials Processing; Surface Engineering-Materials Science

Keywords: Sm_2AlTaO_7; thermal barrier coatings; thermal properties; phase stability

1. Introduction

The 7–8 wt. % yttria (7–8 YSZ) thermal barrier coatings (TBCs) by electron-beam physical vapor deposition (EB-PVD) or air plasma spraying (APS) have attracted extensive interest owing to their applications in metal components of advanced gas turbines (Hardwicke & Lau, 2013; Kumar & Balasubramanian, 2016). However, the YSZ coating has limited temperature capability due to accelerated sintering and phase transformation during long-term operation above 1,473°K (Angle, Steppan, & Thompson, 2014; Limarga, Shian, & Leckie, 2014). As a result, it is very urgent to identify novel ceramic materials with remarkably lower thermal conductivity, proper thermal expansion coefficient, and excellent phase stability between room temperature and operating temperature for TBCs applications (Ren, Wan, Zhao, Yang, & Pan, 2015; Wang & Wang, 2015; Zhang et al., 2015).

During the last decades, the $Ln_2B_2O_7$-type (Ln = rare earth elements, B = Zr, Ce, Sn) oxides have been proposed as potential TBC candidates due to their excellent thermophysical properties (Feng, Xiao, Zhou, & Pan, 2013; Fergus, 2014; Joulia, Vardelle, & Rossignol, 2013; Liu, Wang, Li, & Zhou,

ABOUT THE AUTHORS

Dr Zhang Hongsong, professor is in department of mechanical engineering at Henan Engineering Institute in China. He received his PhD degree in Materials Science at School of Materials Science and Engineering, Beijing Institute of Technology (2007). His current research interest focuses on advanced ceramic materials for thermal barrier coatings, novel ceramic photo-catalysts. The research reported in this paper relates to understanding of a novel ceramic candidate for thermal barrier coatings.

PUBLIC INTEREST STATEMENT

In this paper, a novel pyrochlore-type Sm_2AlTaO_7 oxide which can be used for thermal barrier coatings was prepared by solid state reaction method. The synthesized Sm_2AlTaO_7 has low thermal conductivity, moderate thermal expansion coefficient, and excellent phase stability.

2010; Wang, Guo, Zhang, Gong, & Guo, 2015; Wang & Wang, 2015; Zhang, Shi, Zhao, Li, & Li, 2015). For example, the thermal conductivities of element doped $Ln_2Zr_2O_7$ lie in the range of 1.4–1.65 W m^{-1} K, and their thermal expansion coefficients are close to that of YSZ (Fergus, 2014; Joulia et al., 2013; Ren et al., 2015; Wang & Wang, 2015; Wang et al., 2015; Zhang et al., 2015). The thermal expansion coefficients of $Ln_2Sn_2O_7$ (Ln = La, Nd, Sm, Gd, Er and Yb) oxides are in the same order with that of YSZ, while their thermal conductivities are greater than that of YSZ (Feng et al., 2013). The thermophyscial properties of $Ln_2Hf_2O_7$ were only studied by first principles calculations, and experimental results are still rare (Liu et al., 2010). The $Ln_2Ce_2O_7$ oxides have low thermal conductivities, and their expansion coefficients are higher than that of corresponding $Ln_2Zr_2O_7$ oxides (Zhang, Lv, Li, Zhang, & Wang, 2012; Zhang et al., 2015). In light of the judgmental criterion proposed by Clarke, the low thermal conductivity of the $Ln_2B_2O_7$ oxides can be mainly ascribed to the complex crystal structure, relatively high atomic weight (Clarke, 2003).

Except $A_2B_2O_7$-type oxides, pyrochlore-type oxides and their related compounds with general formula $A_2^{3+}B_1^{3+}B_2^{5+}O_7$ are an important class of materials that possess excellent physicalchemical properties and technological applications (Hinastu & Doi, 2016; Leticia et al., 2012; Li, Chen, Zhang, & Li, 2009; Shlyakhtina et al., 2014; Teixeira, Otubo, Gouveia, & Alves, 2010). For example, Leticia et al. reported the synthesis of Sm_2FeTaO_7 by both solid state reaction and sol–gel routes, and found that Sm_2FeTaO_7 prepared by sol–gel was obtained with lower particle sizes than the solid state produced compound (Leticia et al., 2012). Xuan et al. has synthesized the La_2AlTaO_7 and La_3TaO_7 by solid reaction method using La_2O_3, Al_2O_3, and Ta_2O_5 as raw materials, and found that the photocatalytic activity of La_2AlTaO_7 is higher than that of La_3TaO_7 (Li et al., 2009). Powders and films of Bi_2LnNbO_7 (Ln = In and Al) with pyrochlore-type structures obtained by metal-organic decomposition process are uniform, with nanometric dimensions and high UV–vis transmittance (Teixeira et al., 2010). Hinastu et al. studied the magnetic susceptibility and specific heat of Pr_2YRuO_7 and La_2TbRuO_7 (Hinastu & Doi, 2016). Shlykhtina et al. found that fluorite-like Ho_2ScNbO_7 was obtained at 1,773 and 1,873 K, fluorite-like Ho_2LuNbO_7 is stable in the temperature range 1,473–1,873 K, while pyrochlore-type Sm_2ScTaO_7 exists in the range 1,473–1,673 K (Shlyakhtina et al., 2014). However, the thermophysical properties of the $A_2^{3+}B_1^{3+}B_2^{5+}O_7$ oxides have not been reported in open literatures. In the current manuscript, the Sm_2AlTaO_7 was prepared by solid state reaction, its phase structure and thermophyscial properties were investigated.

2. Experimental

The Sm_2AlTaO_7 was synthesized by solid reaction method using Sm_2O_3 (≥99.9%), Al_2O_3 (≥99.9%) and Ta_2O_5 (≥99.9%) as the starting reactants. Firstly, these raw oxides were fired at 1173 K for 3 h before weighting the stoichiometric constituent of Sm_2AlTaO_7. Secondly, these oxides were mixed by ball milling for 6 h and dried at 293 K overnight, and the obtained mixing powders were pressed into disk pellets at 100 PMa pressure. Thirdly, the sintering process of Sm_2AlTaO_7 pellets was repeated three times at 1,673 K for 10 h. Finally, the pressed pellets were calcined and reacted at 1,873 K for 30 h to achieve corresponding bulk samples.

The phase structure of bulk samples was characterized by X-ray diffraction (XRD, Bruker D8 Advance diffractometer). The actual bulk density (ρ) was measured by Archimedes drainage method, and the microstructure of the bulk samples was observed via scanning electron microscope (SEM, FEI Quanta-250). In the range of 293–1,273 K, the thermal diffusivity (λ) testing of Sm_2AlTaO_7 was carried out using a laser flash apparatus (Linseis LFA1000, Germany) in an argon atmosphere. The sample size for thermal diffusivity measurement is about Φ 12.7 × 2 mm, and the front and back surfaces of the sample were coated with a graphic thin layer in order to prevent the laser penetrating through the translucent sample at high temperatures. The specific heat capacity (C_p) of Sm_2AlTaO_7 was calculated by the Neumann–Kopp rule based on the heat capacities of the constituent oxides (Sm_2O_3, Al_2O_3, and Ta_2O_5) (Swalin, 1972). The thermal conductivity (k) of Sm_2AlTaO_7 was achieved in light of Equation (1), which was further revised into the actual value (k_0) using Equation (2) in order to remove the influence of porosity (φ). Its thermal expansion coefficient (TEC) between ambient

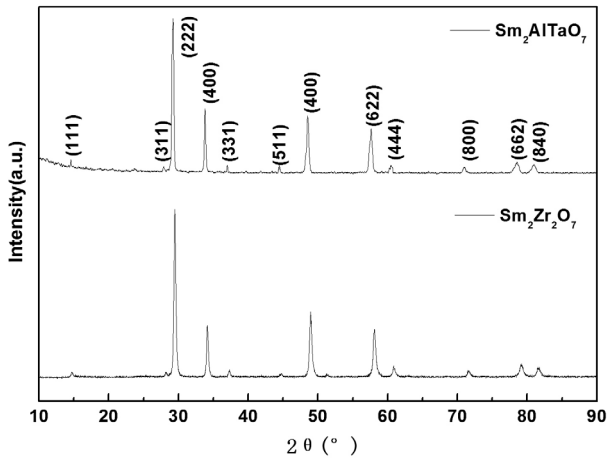

Figure 1. XRD patter of Sm_2AlTaO_7 oxide.

and 1,273 K was determined with a high temperature dilatometer (Netzsch DIL402C/7, Germany). The phase stability was investigated using differential scanning calorimetry (DSC, Netzsch STA449-F3, Germany) from ambient temperature to 1,673 K under high pure N_2.

$$k = C_p \cdot \rho \cdot \lambda \tag{1}$$

$$\frac{k}{k_0} = 1 - \left(\frac{4}{3}\right)\varphi \tag{2}$$

3. Results and discussion

3.1. XRD

Figure 1 lists the XRD patterns of Sm_2AlTaO_7 together with the data of $Sm_2Zr_2O_7$. Clearly, it can be observed that the diffraction peaks of Sm_2AlTaO_7 match well with that of pyrochlore-type $Sm_2Zr_2O_7$. Therefore, the Sm_2AlTaO_7 shows a typical pyrochlore-type structure, which is also characterized by the presence of typical superstructure peaks at 2θ values of about 29.697 (311), 31.33 (222), 40.091 (331), and 46.658 (511). It also can be seen from Figure 1 that no other peaks can be found in the product, which means that pure pyrochlore-type Sm_2AlTaO_7 is synthesized successfully.

3.2. Microstructure

Figure 2(a) presents the typical micro-morphology of Sm_2AlTaO_7. SEM observation shows that its average grain size is several micrometers. The microstructure is very dense, only a few apparent micropores are detected. The grain boundaries of the synthesized oxide are very clean, no other phases or un-reacted oxides exist in the interfaces. Its actual density is 5.28 g cm^{-3}, and the relative density is about 94.5%, which illustrates that the sintered sample can be used for further examination of thermophysical properties. The element compositions analyzed by EDS are displayed in Figure 2(b) and Table 1. Obviously, the Sm_2AlTaO_7 is composed of Sm–Al–Ta–O, and the atomic ratio value of n_{Sm}:n_{Al}:n_{Ta} is almost 2:1:1, which is consistent with the theoretical composition of Sm_2AlTaO_7.

3.3. Thermophysical property

As can be noted from Figure 3, the DSC curve of Sm_2AlTaO_7 is smooth, and there are no exothermic or endothermic peaks above 773 K. This phenomenon indicates that Sm_2AlTaO_7 displays excellent phase stability in the range of 773–1,673 K. The small peak at about 500°C may be ascribed to the vibration of the testing instrument. Figure 4 shows the temperature dependence of the specific heat capacity of Sm_2AlTaO_7. Clearly, the specific heat capacity increases with the increasing temperature up to 1,473 K, which can be fitted by the following equations.

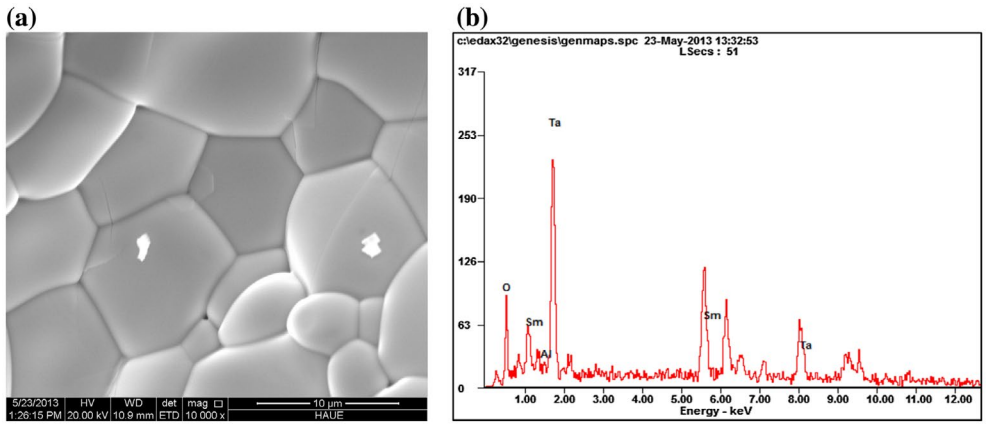

Figure 2. (a) Microstructure of as-prepared Sm_2AlTaO_7 oxide; (b) EDS pattern of Sm_2AlTaO_7.

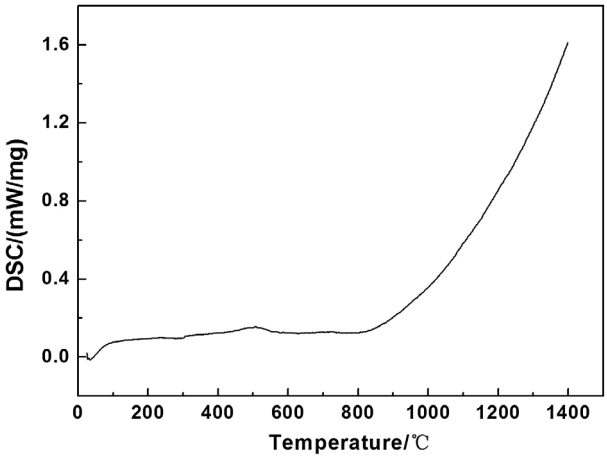

Figure 3. DSC curve of Sm_2AlTaO_7 oxide.

Table 1. Element atomic ratio of Sm_2AlTaO_7

Element atomic	Sm	Al	Ta	O
Sm_2AlTaO_7	22.06	11.45	12.94	53.55

$$C_P(Sm_2AlTaO_7) = 0.41356 + 0.00008 \times T - 7076.27528/T^2 \quad (3)$$

The temperature-dependence curves of thermal diffusivity and thermal conductivity of Sm_2AlTaO_7 oxide are displayed in Figure 5. Clearly, the thermal diffusivity manifests an inverse temperature-dependence, and the T^{-1}-dependence thermal diffusivity suggests an obvious phonon conduction behavior. With the increasing temperature, its thermal conductivity decreases from 1.95 to 1.13 W m^{-1} K^{-1} in the range of 473–1,273 K. Its thermal conductivity is much lower than that of YSZ (Zhang et al., 2009) and $Sm_2Ce_2O_7$ (Chen, Yang, Zhang, Li, & Li, 2014). According to the phonon thermal conductivity theory, the lattice thermal conductivity of the electric-insulation ceramics can be reduced by the phonon scattering resulted by the lattice point defect, such as substituting atoms, vacancies, and dislocations (Klemens, 2002; Wachsman, 2004). The Sm_2AlTaO_7 can be regarded as the substitutional solid solution, which are formed by the substitution of Ta^{5+} cation by trivalent Sm^{3+} and Al^{3+} ions when trivalent cations are doped into Ta_2O_5 (Khaw, Tan, Lee, & West, 2012; Tan, Khaw, Lee, Zainal, & Miles, 2010; Vanderah, Guzman, Nino, & Roth, 2008). The substitution of Ta^{5+} cations

Figure 4. Specific heat capacity of Sm_2AlTaO_7 oxide.

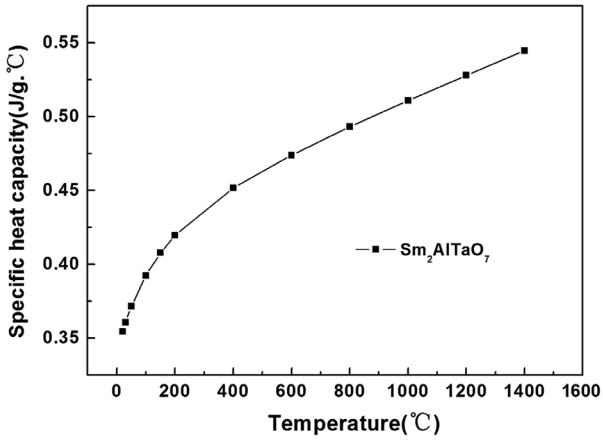

Figure 5. Thermal diffusivity and thermal conductivity of Sm_2AlTaO_7 oxide.

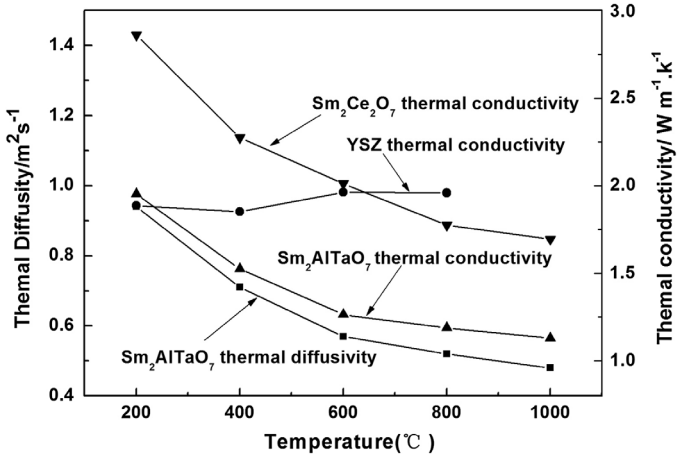

with Ln^{3+} cations (Ln = Sm and Al) is accompanied by the oxygen vacancies, to maintain the local electro-neutrality of the lattice. The defect chemistry due to co-doping can be expressed using the Kröger–Vink notation by the following equation, Ln''_{Ta} represents an Ln^{3+} cation that occupies a Ta^{5+} cation site (divalent negative charge), $V_o^{\cdot\cdot}$ is a doubly charged oxygen vacancy, and O_o^x is an O^{2-} anion on an oxygen site (neutral charge). Ln in Equation (4) can be either Sm and Al. Clearly, the concentration of oxygen vacancies in

Figure 6. Thermal expansion coefficient of Sm_2AlTaO_7 ceramic.

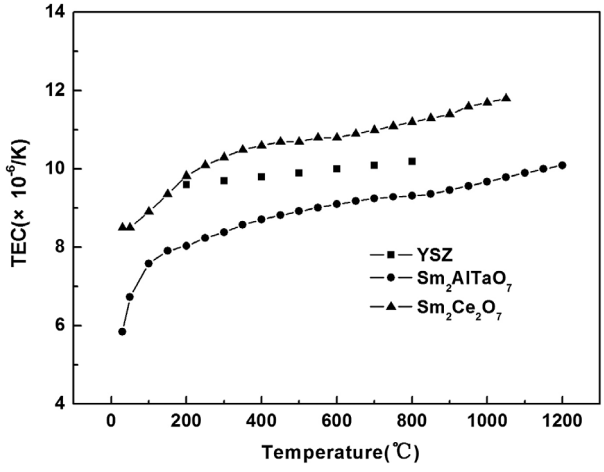

$$Ln_2O_3 \xrightarrow{Ta_2O_5} 2Ln''_{Ta} + 2V_o^{\cdot\cdot} + 3O_o^x \quad (4)$$

Sm_2AlTaO_7 is significantly greater than that of 8YSZ. Therefore, the synthesized ceramics has lower thermal conductivity as compared to 8YSZ due to the scattering of the phonons by the oxygen vacancies.

According to the phonon thermal conduction theory, the thermal conductivity is proportional to the phonon mean free path, and the influence of substituting atoms on phonon free path (l_p) can be expressed by Equation (1) (Chen et al., 2014):

$$\frac{1}{l_p} = \frac{a^3}{4\pi v^4}\omega^4 c\left(\frac{\Delta M}{M}\right)^2 \quad (5)$$

where a^3 is the volume per atom, v the transverse wave speed, ω the phonon frequency, c the concentration per atom, M the average mass of the host atom, ΔM the differences of masses between the substituted and substituting atoms, respectively. The atomic weights of samarium, aluminum, and tantalum are 150.9, 26.9, and 180.9, which means the atomic mass difference between A site and B site is very great. The effective phonon scattering by atomic mass difference contributes the low thermal conductivity. In addition, the low thermal conductivity can also be attributed to its high level of local disorder in crystal structure and bonding character, which can increase a harmonic interaction among phonons effectively (Klemens, 2002).

Its thermal expansion coefficient is presented in Figure 6. Its TEC increases smoothly with the temperature reaching 1,473 K. Its TEC at 1,200°C is about 10.1×10^{-6}/K, which is obviously lower than that of $Sm_2Ce_2O_7$ (11.09×10^{-6}/K) (Joulia et al., 2013), but close to that of YSZ (10.6×10^{-6}/K). According to the thermal expansion theory, a low strength of ionic bond often leads to a great ionic distance, that is, a high TEC can be obtained. The strength of ionic bond is given as Equation (2) (Wachsman, 2004):

$$I_{A-B} = 1 - e^{-\frac{(x_A - x_B)^2}{4}} \quad (2)$$

where $I_{A\text{-}B}$ is the intensity of ionic bond between ions at A site and B site, x_A and x_B are the average electro-negativity of ions at A site and B site. Therefore, a low electronegativity difference between cations at site A and B contributes to the TEC reduction. Electronegativities of Sm, Al, Ta, and Ce are 1.17, 1.61, 1.5, and 1.12. Thus, the electronegativity difference between cations at A site for Sm_2AlTaO_7 is higher than that of $Sm_2Ce_2O_7$, which contributes to the lower thermal expansion coefficient as compared with $Sm_2Ce_2O_7$.

4. Conclusions

(1) The pure Sm_2AlTaO_7 with single pyrochlore structure was prepared, this oxide is thermally stable in the temperature range of 293–1,673 K.

(2) Its thermal conductivity is 1.13 W m^{-1} K^{-1} at 1,273 K, which is much lower than that of YSZ. The lower thermal conductivity can be attributed to the phonon scattering resulted by substituted atoms and local lattice distortion.

(3) Its average TEC is moderate, which is lower than that of $Sm_2Ce_2O_7$, but close to that of YSZ. The moderate TEC can be ascribed to the relative higher electronegativities of Al and Ta cations.

(4) The synthesized Sm_2AlTaO_7 has a promising future for TBCs.

Funding
The authors would like to thank the financial support from the Projects National Nature Foundation of China [grant number U1304512]; Program for science &Technology Innovation Talents in Universities of Henan Province [grant number 13HASTIT018]; the Scientific and Technological Projects of Henan Province [grant number 132102210142] and the Postdoctoral Research Sponsorship in Henan Province [grant number 2014069].

Author details
Yu Haipeng[1]
E-mail: haipengyu@126.com
Chen Xiaoge[2]
E-mail: chenxg831025@163.com
Zhang Hongsong[3,4]
E-mail: zhsandchen@126.com
Zhang Haoming[4]
E-mail: haoming@126.com
Zhao Yongde[3]
E-mail: yongde@126.com
Liu Yanxu[4]
E-mail: yanxu@126.com
Tang An[4]
E-mail: antang@126.com
[1] School of Textile Engineering, Henan Institute of Engineering, Zhengzhou 450002, China.
[2] School of Civil Engineering, Henan Institute of Engineering, Zhengzhou 450002, China.
[3] Institute of Chemistry, Henan Academy of Sciences, Zhengzhou 450007, China.
[4] School of Mechanical Engineering, Henan Institute of Engineering, Zhengzhou 450002, China.

Citation information
Cite this article as: Preparation and thermal properties of Sm_2AlTaO_7, Yu Haipeng, Chen Xiaoge, Zhang Hongsong, Zhang Haoming, Zhao Yongde, Liu Yanxu & Tang An, *Cogent Physics* (2016), 3: 1244244.

References

Angle, J. P., Steppan, J. J., & Thompson, P. M. (2014). Parameters influencing thermal shock resistance and ionic conductivity of 8 mol% yttria-stabilized zirconia (8YSZ) with dispersed second phases of alumina or mullite. *Journal of the European Ceramic Society, 34*, 4327–4336. doi:10.1016/j.jeurceramsoc.2014.06.020

Chen, X. G., Yang, S. S., Zhang, H. S., Li, G., & Li, Z. J. (2014). Preparation and thermophysical properties of $(Sm_{1-x}Er_x)_2Ce_2O_7$ oxides for thermal barrier coatings. *Materials Research Bulletin, 47*, 4181–4186. doi:10.1016/j.materresbull.2013.12.011

Clarke, D. R. (2003). Materials selection guidelines for low thermal conductivity thermal barrier coatings. *Surface and Coatings Technology, 163*, 67–74. doi:10.1016/S0257-8972(02)00593-5

Feng, J., Xiao, B., Zhou, R., & Pan, W. (2013). Thermal expansion and conductivity of $RE_2Sn_2O_7$ (RE=La, Nd, Sm, Gd, Er and Yb) pyrochlores. *Scripta Materialia, 69*, 401–404. doi:10.1016/j.scriptamat.2013.05.030

Fergus, J. W. (2014). Zirconia and pyrochlore oxides for thermal barrier coatings in gas turbine engines. *Metallurgical and Materials Transactions E, 1*, 118–131. doi:10.1007/s40553-014-0012-y

Hardwicke, C. U., & Lau, Y. C. (2013). Advances in thermal spray coatings for gas turbines and energy generation: A review. *Journal of Thermal Spray Technology, 22*, 564–576. doi:10.1007/s11666-013-9904-0

Hinastu, Y., & Doi, Y. (2016). Structures and magnetic properties of new fluorite-related quaternary rare earth oxides LnY_2TaO_7 and $LaLn_2RuO_7$ (Ln= rare earths). *Journal of Solid State Chemistry, 233*, 37–43. doi:10.1016/j.jssc.2015.10.1012

Joulia, A., Vardelle, M., & Rossignol, S. (2013). Synthesis and thermal stability of $Re_2Zr_2O_7$, (Re=La, Gd) and $La_2(Zr_{1-x}Ce_x)_2O_7$.δ compounds under reducing and oxidant atmospheres for thermal barrier coatings. *Journal of the European Ceramic Society, 33*, 2633–2644. doi:10.1016/j.jeurceramsoc.2013.03.030

Khaw, C. C., Tan, K. B. C., Lee, C. K., & West, A. R. (2012). Phase equilibria and electrical properties of pyrochlore and zirconolite phases in the Bi_2O_3–ZnO–Ta_2O_5 system. *Journal of the European Ceramic Society, 32*, 671–680. doi:10.1016/j.jeurceramsoc.2011.10.1012

Klemens, P. G. (2002). Effect of point defects on the decay of the longitudinal optical mode. *Physica B: Condensed Matter, 316–317*, 413–416. doi:10.1016/S0921-4526(02)00530-6

Kumar, V., & Balasubramanian, K. (2016). Progress update on failure mechanisms of advanced thermal barrier coatings: A review. *Progress in Organic Coatings, 90*, 54–82. doi:10.3724/SP.J.1077.2012.11565

Leticia, T. M., Miguel, A. R. G., Torrres, M. F., Isaias, J. R., Edgar, M., & Enrique, L. C. (2012). Synthesis by two methods and crystal structural determination of a new pyrochlore related compound Sm_2FeTaO_7. *Materials Chemistry and Physics, 133*, 839–844. doi:10.1016/j.matchemphys.2012.01.104

Li, Y. X., Chen, G., Zhang, H. J., & Li, Z. H. (2009). Photocatalytic water splitting of La_2AlTaO_7 and the effect of aluminum on the electronic structure. *Journal of Physics and Chemistry of Solids, 70*, 536–540. doi:10.1016/j.jpcs.2008.12.005

Limarga, A. M., Shian, S., & Leckie, R. M. (2014). Thermal conductivity of single and multi-phase compositions in the ZrO_2-Y_2O_3-Ta_2O_5 system. *Journal of the European Ceramic Society, 34*, 3085–3094. doi:10.1016/j.jeur-ceramsoc.2014.03.013

Liu, B., Wang, J. Y., Li, F. Z., & Zhou, Y. C. (2010). Theoretical elastic stiffness, structural stability and thermal conductivity of $La_2T_2O_7$ (T=Ge, Ti, Sn, Zr, Hf) pyrochlore. *Acta Materialia, 58*, 4369–4377. doi:10.1016/j.actamat.2010.04.031

Ren, X. R., Wan, C. L., Zhao, M., Yang, J., & Pan, W. (2015). Mechanical and thermal properties of fine-grained quasi-eutectoid $(La_{1-x}Yb_x)_2Zr_2O_7$ ceramics. *Journal of the European Ceramic Society, 35*, 3145–3154. doi:10.1016/j.jeurceramsoc.2015.04.024

Shlyakhtina, A. V., Belov, D. A., Pigalskiy, K. S., Shchegolikhin, A. N., Kolbanev, I. V., & Karyagina, O. K. (2014). Synthesis, properties and phase transitions of pyrochlore- and fluorite-like Ln_2RMO_7 (Ln=Sm, Ho; R=Lu, Sc; M=Nb, Ta). *Materials Research Bulletin, 49*, 625–632. doi:10.1016/j.materresbull.2013.10.004

Swalin, R. A. (1972). *Thermodynamics of solids* (pp. 53–87). New York, NY: John Wiley & Sons Press.

Tan, K. B., Khaw, C. C., Lee, C. K., Zainal, Z., & Miles, G. C. (2010). Structures and solid solution mechanisms of pyrochlore phases in the systems Bi_2O_3–ZnO–$(Nb, Ta)_2O_5$. *Journal of Alloys and Compounds, 508*, 457–462. doi:10.1016/j.jallcom.2010.08.093

Teixeira, Z., Otubo, L., Gouveia, R. F., & Alves, O. L. (2010). Preparation and characterization of powders and thin films of Bi_2AlNbO_7 and Bi_2InNbO_7 pyrochlore oxides. *Materials Chemistry and Physics, 124*, 552–557. doi:10.1016/j.matchemphys.2010.07.009

Vanderah, T. A., Guzman, J. L., Nino, J. C., & Roth, R. S. (2008). Stability phase-fields and pyrochlore formation in sections of the Bi 2O3 -Al2O3 -Fe 2O3 -Nb2O5 system. *Journal of the American Ceramic Society, 91*, 3659–3662. doi:10.1111/j.1551-2916.2008.02648

Wachsman, E. D. (2004). Effect of oxygen sublattice order on conductivity in highly defective fluorite oxides. *Journal of the European Ceramic Society, 24*, 1281–1285. doi:10.1016/S0955-2219(03)00509-0

Wang, X. Z., Guo, L., Zhang, H. L., Gong, S. K., & Guo, H. B. (2015). Structural evolution and thermal conductivities of $(Gd_{1-x}Yb_x)_2Zr_2O_7$ (x=0, 0.02, 0.04, 0.06, 0.08, 0.1) ceramics for thermal barrier coatings. *Ceramics International, 41*, 12621–12625. doi:10.1016/j.ceramint.2015.06.090

Wang, C. J., & Wang, Y. (2015). Thermophysical properties of $La_2(Zr_{0.7}Ce_{0.3})_2O_7$ prepared by hydrothermal synthesis for nano-sized thermal barrier coatings. *Ceramics International, 41*, 4601–4607. doi:10.016/j.ceramint.2014.12.003

Zhang, H. S., Lv, J. G., Li, G., Zhang, Z., & Wang, X. L. (2012). Investigation about thermophyscial properties of $Ln_2Ce_2O_7$ (Ln=Sm, Er, and Yb) oxides for thermal barrier coatings. *Materials Research Bulletin, 47*, 4181–4186. doi:10.1016/j.materresbull.2012.08.074

Zhang, H. S., Shi, L., Zhao, Y. D., Li, G., & Li, Z. J. (2015). Thermal conductivities and thermal expansion coefficients of $(Sm_{0.5}Gd_{0.5})_2(Ce_{1-x}Zr_x)_2O_7$ ceramics. *Journal of Materials Engineering and Performance, 23*, 3394–3399. doi:10.1007/s11665-015-1621-z

Zhang, Y. H., Xie, M., Zhou, F. X., Cui, X., Lei, X. G., Song, X. W., & An, S. L. (2015). Influence of Er substitution for La on the thermal conductivity of $(La_{1-x}Er_x)_2Zr_2O_7$ pyrochlores. *Materials Research Bulletin, 64*, 175–181. doi:10.1016/j.materresbull.2014.12.064

Zhang, H. S., Xu, Q., Wang, F. C., Liu, L., Wei, Y., & Chen, X. G. (2009). Preparation and thermophyscial properties of $(Sm_{0.5}La_{0.5})_2Zr_2O_7$ and $(Sm_{0.5}La_{0.5})_2(Zr_{0.8}Ce_{0.2})_2O_7$ ceramics for thermal barrier coatings. *Journal of Alloys and Compounds, 475*, 624–628. doi:10.1016/j.jallcom.2008.07.068

***Cogent Physics* (ISSN: 2331-1940) is published by Cogent OA, part of Taylor & Francis Group.**